Published OnlineFirst January 3, 2014; DOI: 10.1158/1078-0432.CCR-13-1642

Clinical Cancer Research

Imaging, Diagnosis, Prognosis

Ultrasound Molecular Imaging in a Human CD276 Expression–Modulated Murine Ovarian Cancer Model

Amelie M. Lutz[1], Sunitha V. Bachawal[1], Charles W. Drescher[4], Marybeth A. Pysz[1], Jürgen K. Willmann[1,3], and Sanjiv Sam Gambhir[1,2,3]

Abstract

Purpose: To develop a mouse ovarian cancer model that allows modulating the expression levels of human vascular targets in mouse xenograft tumors and to test whether expression of CD276 during tumor angiogenesis can be visualized by molecularly targeted ultrasound *in vivo*.

Experimental Design: CD276-expressing MILE SVEN 1 (MS1) mouse endothelial cells were engineered and used for coinjection with 2008 human ovarian cancer cells for subcutaneous xenograft tumor induction in 15 nude mice. Fourteen control mice were injected with 2008 cells only. After confirming their binding specificity in flow chamber cell attachment studies, anti-CD276 antibody-functionalized contrast microbubbles were used for *in vivo* CD276-targeted contrast-enhanced ultrasound imaging.

Results: CD276-targeted ultrasound imaging signal was significantly higher ($P = 0.006$) in mixed MS1/2008 tumors than in control tumors. Compared with control microbubbles, the ultrasound signal using CD276-targeted microbubbles was significantly higher ($P = 0.002$), and blocking with purified anti-CD276 antibody significantly decreased ($P = 0.0096$) the signal in mixed MS1/2008 tumors. Immunofluorescence analysis of the tumor tissue confirmed higher quantitative immunofluorescence signal in mixed MS1/2008 tumors than in control 2008 only tumors, but showed not significantly different ($P = 0.54$) microvessel density.

Conclusions: Our novel small animal model allows for modulating the expression of human tumor–associated vascular endothelial imaging targets in a mouse host and these expression differences can be visualized noninvasively by ultrasound molecular imaging. The animal model can be applied to other human vascular targets and may facilitate the preclinical development of new imaging probes such as microbubbles targeted at human vascular markers not expressed in mice. *Clin Cancer Res; 20(5); 1313–22. ©2014 AACR.*

Introduction

Ovarian cancer is the most lethal of all the gynecologic malignancies and the 5th overall leading cause of cancer-related deaths in women (1). Ovarian cancer frequently remains asymptomatic until the disease has far progressed; when symptoms develop they are often nonspecific and lead to clinical evaluation for other more common illnesses, which delays the diagnosis even further. Perhaps the greatest opportunity for improving ovarian cancer outcomes is through earlier detection of the disease, because overall ovarian cancer 5-year survival is 50%, but can be 90% when the disease is confined to the ovary at diagnosis; however, only 30% of cases are diagnosed in this early stage (2, 3). When ovarian cancer is finally suspected, pelvic imaging using transvaginal sonography (TVS) is the most common first-line diagnostic test. Conventional TVS, unfortunately, offers limited sensitivity and specificity in detection of ovarian cancer hampering its use as a screening tool for early detection (4–6). Outcomes for women with or at risk for ovarian cancer could likely be substantially improved by advances in imaging methods, especially TVS, for detecting the disease.

Molecularly targeted contrast-enhanced ultrasound (CEUS) offers great potential for improving sensitivity and/or specificity of TVS for earlier detection of ovarian cancer. Recent studies in mouse xenograft tumor models showed promising results using the angiogenesis marker VEGFR2 as an imaging target in molecularly targeted CEUS, allowing detection of cancer-specific imaging signal in tumors as small as 2-mm diameter (7–12). Despite these promising results in the tumor xenograft setting and the

Authors' Affiliations: Departments of [1]Radiology and [2]Bioengineering and Materials Science and Engineering; [3]Molecular Imaging Program at Stanford, Stanford University School of Medicine, Stanford, California; and [4]Division of Public Health Sciences, Fred Hutchinson, Cancer Research Center, Seattle, Washington

Note: Supplementary data for this article are available at Clinical Cancer Research Online (http://clincancerres.aacrjournals.org/).

Corresponding Author: Sanjiv Sam Gambhir, Stanford University School of Medicine, Stanford, CA 94305. Phone: 650-384-5142; Fax: 650-724-4948; E-mail: sgambhir@stanford.edu

doi: 10.1158/1078-0432.CCR-13-1642

Published OnlineFirst January 3, 2014; DOI: 10.1158/1078-0432.CCR-13-1642

Translational Relevance

Extensive research is under way to identify novel tumor vascular–associated biomarkers. Small animal models are a requisite for the development of novel drugs, including contrast agents and molecular imaging probes, but not all novel human tumor biomarkers of interest are reliably expressed in mouse tumor models. The proposed animal model allows modulation of the expression of a human ovarian cancer–associated vascular biomarker on tumor-associated vascular endothelial cells in the mouse host. Furthermore, these differences in biomarker expression on vascular endothelial cells can be assessed with molecularly targeted ultrasound imaging. This novel small animal model may be applicable to many human vascular tumor biomarkers and may facilitate not only the development of imaging probes targeted at newly described vascular imaging biomarkers for cancer, but may also be helpful in the development of novel therapeutics targeted at those vascular biomarkers.

potential of being a suitable imaging target in the majority of patients with postmenopausal ovarian cancer, VEGFR2 may not be an entirely optimal target for the detection of ovarian cancer in the subset of patients with premenopausal ovarian cancer. VEGFR2 is not a cancer-specific angiogenesis marker and expression levels are known to be upregulated on vascular endothelial cells at sites of wound healing, which also regularly occurs in the ovary in the early luteal phase following ovulation (13). Therefore, a concern is that imaging strategies targeting VEGFR2 for earlier ovarian cancer detection may result in false positives when scanning the ovary during physiologic angiogenesis associated with ovulation in premenopausal women. Imaging targets that are specifically upregulated on tumor-associated vascular endothelial cells are therefore highly desirable for molecularly targeted CEUS in the setting of ovarian cancer. Extensive research is under way aiming at identifying cancer-specific vascular markers for numerous cancers, including ovarian cancer, for therapeutic and diagnostic purposes (14–17). A drawback of many of these biomarkers, is the often limited (or even lack of) expression of the vascular markers in mouse tumor models, especially subcutaneous xenografts. However, mouse tumor models represent an often necessary and cost-effective first step in the development of drugs and imaging agents targeting these novel vascular markers. One more cancer-specific ovarian cancer–associated vascular endothelial marker, CD276 (B7-H3), a member of the immunoglobulin superfamily had recently been identified by our collaborators by data mining of gene expression data banks and confirmed as a promising imaging target for ovarian cancer after immunohistopathology validation in human early stage ovarian cancer samples. CD276 vascular expression was identified in a majority of serous ovarian cancer tissues and in only a minority of tissue samples from corpus luteum and benign ovarian tumors (C. Drescher et al., unpublished data). The importance of CD276 as a vascular marker in ovarian and other cancers has also been confirmed by other authors (16–19). CD276 may be a suitable molecular imaging target in ovarian cancer, especially in the setting of a multivalent imaging approach targeting 2 or more complementary tumor markers simultaneously (7). Although, expression of murine CD276 in tumor-associated mouse vasculature had been described in the past, we could only find very low expression levels of this marker on tumor-associated vascular endothelial cells in our mouse ovarian cancer xenograft models (unpublished data). Following the concept that endothelial cells can form tubular three-dimensional structures that can connect to host capillary microcirculation (20), we attempted to create an animal model that is suitable for use in a high-throughput multiuser molecular imaging laboratory environment.

Our goal was to establish a novel mouse xenograft tumor model that allows upregulation of the expression of human vascular markers such as human CD276 on tumor-associated vascular endothelial cells and to evaluate whether the differences in human CD276 expression can be visualized by molecularly targeted CEUS imaging.

Materials and Methods

Creation of CD276 expressing stable mouse endothelial cells

MILE SVEN 1 (MS1) mouse vascular endothelial cells [CRL2279; American Type Culture Collection (ATCC)] were transfected with human *CD276* after confirming the absence of CD276 expression on these cells via Western blot analysis. Wild-type MS1 cells (WT MS1) were subcultured under sterile conditions and maintained in a 5% CO_2 -humidified atmosphere at 37°C until needed for the experiments in ATCC-formulated Dulbecco's Modified Eagle Medium (ATCC) with FBS at 5%.

For the creation of stable CD276-expressing MS1 cell clones ($MS1_{CD276}$), an expression-optimized version of the gene encoding for human *CD276* (DNA2.0, sequence see Supplementary Appendix, $CD276_{engineered}$) was subcloned into an ubiquitin promoter–driven expression vector for further use (see Supplementary Appendix for detailed protocol).

Transfection of MS1 cells with the *CD276*-expression vector was performed using lipofectamine 2000 transfection reagent (Life Sciences; Invitrogen), following the recommended manufacturer's standard protocol (ref. 21; see Supplementary Appendix). One transfected MS1 clone was found to show particularly high CD276 expression (Fig. 1). Of note, the anti-CD276 monoclonal antibody (mAb) cross-reacts with human and mouse CD276 and can, therefore, not differentiate between the 2 protein versions.

Preparation of CD276-targeted and control microbubbles for imaging

Commercially available lipid-shelled, perfluorocarbon-containing microbubbles (Vevo MicroMarker Target Ready

Published OnlineFirst January 3, 2014; DOI: 10.1158/1078-0432.CCR-13-1642

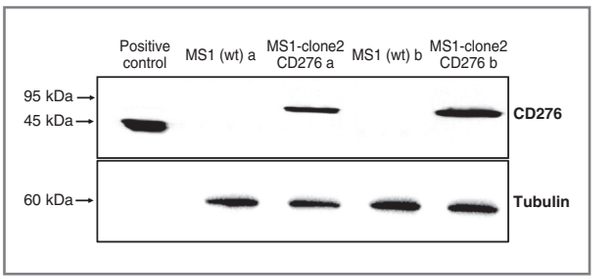

Figure 1. Testing of CD276 expression in transfected MS1 cells. Western blot of samples deriving from truncated recombinant CD276 (positive control, purified, 40–45 kDa under reducing conditions; R&D Systems), wild-type MS1 cell lysates [MS1(wt) a and MS1(wt) b] as well as lysates of MS1 clone 2 cells, which were transfected with the CD276 gene (MS1-clone 2 a and b, approximately 95 kDa under reducing conditions) shows expression of CD276 in transfected MS1 cells, but not in wild-type MS1 cells. 15 μg of protein were loaded into lanes MS1(wt) a and MS1-clone 2 CD276 a, respectively. Thirty micrograms of protein were loaded into lanes MS1(wt) b, MS1-clone 2 CD276 b, and positive control.

Contrast Agent Kit; VisualSonics) were used to generate CD276-targeted microbubbles that can serve as a contrast agent for CEUS. Each vial of microbubbles was incubated with 30 μg of anti-mouse/human CD276 biotinylated mAb (eBioscience) diluted in sterile saline according to the microbubble manufacturer's manual allowing the antibody to bind to the microbubbles through streptavidin–biotin interactions; thus, the microbubbles were functionalized with anti-CD276 monoclonal antibodies (MB_{CD276}). Non-targeted reconstituted microbubbles (MB_{Pure} for flow chamber experiments) and isotype-matched control immunoglobulin G antibody (ABD Serotec, 30 μg of Ab per vial of microbubbles) functionalized microbubbles (MB_{Iso}) served as control contrast agents. Figure 2 illustrates the algorithm for the subsequent experiments.

Flow chamber experiments

To assess binding specificity of the CD276-targeted microbubbles to human CD276, microbubble binding was assessed in flow chamber experiments on $MS1_{CD276}$ cells as well as WT MS1 cells (no CD276 expression; ref. 22). A total of 5×10^4 $MS1_{CD276}$ cells or WT MS1 cells were grown on coated (Sigmacote; Sigma-Aldrich) glass microscope slides and mounted on a parallel-plate flow chamber (GlycoTech Corporation). In separate experiments, MB_{CD276}, MB_{pure}, or MB_{Iso} at a concentration of 0.7×10^7 microbubbles per milliliter in PBS were passed over the cells by use of a syringe infusion/withdrawal pump (Genie Plus; Kent Scientific Corporation). A flow rate of 0.6 mL/min (corresponding to a wall shear rate of 100 per second, the approximate shear rate in tumor capillaries; ref. 23) for the microbubbles in PBS was used, which was followed by a 2-minute PBS rinse at the same flow rate. All experiments were performed in triplets.

To further test the binding specificity of MB_{CD276}, additional cell slides were blocked by incubation with an excess of nonbiotinylated anti-CD276 mAb (60 μg for 30 minutes) before performing the flow chamber experiment with MB_{CD276}. The mean number of microbubbles attached per cell in 5 randomly selected optical fields was determined by phase contrast microscopy (at ×400; Axiovert 25; Carl Zeiss AG). Microbubbles can be directly visualized as small, white-rounded structures; microbubbles were considered to be attached to cells when there was direct contact with the cells and no free floating was noted under real-time observation. The number of attached microbubbles and the number of cells were counted to calculate the number of attached microbubbles per cell (22).

Mouse model

All procedures involving the use of laboratory animals were approved by the Institutional Administrative Panel on Laboratory Animal Care at Stanford University. For subcutaneous ovarian cancer xenograft tumor induction, 6-week-old athymic nude mice (Charles River Laboratories) were used. During the injections, the mice were anesthetized with 2% to 3% isoflurane (Aerrane; Baxter) in oxygen administered at a rate of 2 L/min. Human 2008 endometrioid ovarian cancer cells (24) were cultured in RPMI 1640 medium (Life Technologies) with 10% FBS. In pilot experiments, 1×10^6 2008 ovarian cancer cells were mixed with CD276-expressing MS1 ($MS1_{CD276}$) cells at ratios of 1:5 (1×10^6 2008 cells and 5×10^6 $MS1_{CD276}$ cells) and 1:10 (1×10^6 2008 cells and 1×10^7 $MS1_{CD276}$ cells), respectively, resuspended in phenol red–free basement membrane matrix (Matrigel; BD Biosciences) and injected subcutaneously in the right flank. Different ratios of 2008 tumor cells to $MS1_{CD276}$ cells were tried for tumor induction. The coinjection of the cells at a ratio of 1:5 showed optimal CD276 expression levels on tumor-associated vascular endothelial cells and good tumor sizes after 20 days after subcutaneous injection. For subsequent experiments, 2008 cells and $MS1_{CD276}$ cells were always coinjected at a ratio of 1:5 for xenograft tumor induction. When MS1 cells were injected subcutaneously alone in pilot experiments, they grew only very slowly into small flat lesions, resembling hemangiomas (25) and did not develop into the typical round exophytic subcutaneous tumor as the ones grown from either 2008 cells alone or mixed 2008 and MS1 cells.

A total of 15 mice with mixed $MS1_{CD276}$/2008 tumors were used for *in vivo* molecularly targeted CEUS imaging experiments, and an additional 14 animals injected with 3×10^6 2008 cells only serving as negative controls (representative of the typical cell number used for subcutaneous xenograft tumor induction). The number of 3×10^6 of 2008 cells was chosen for the induction of control tumors (control 2008 only tumors), because this cell number had consistently been shown to result in similar sized tumors over a time interval of 3 weeks based on our experience. All tumors were allowed to grow for 19 to 20 days after injection up to a mean maximum size of 5.8 mm (range, 4.4–7.7 mm) for the mixed $MS1_{CD276}$/2008 tumors and of 5.8 mm (range, 3.0–7.8 mm) for the control 2008 only tumors, respectively.

Published OnlineFirst January 3, 2014; DOI: 10.1158/1078-0432.CCR-13-1642

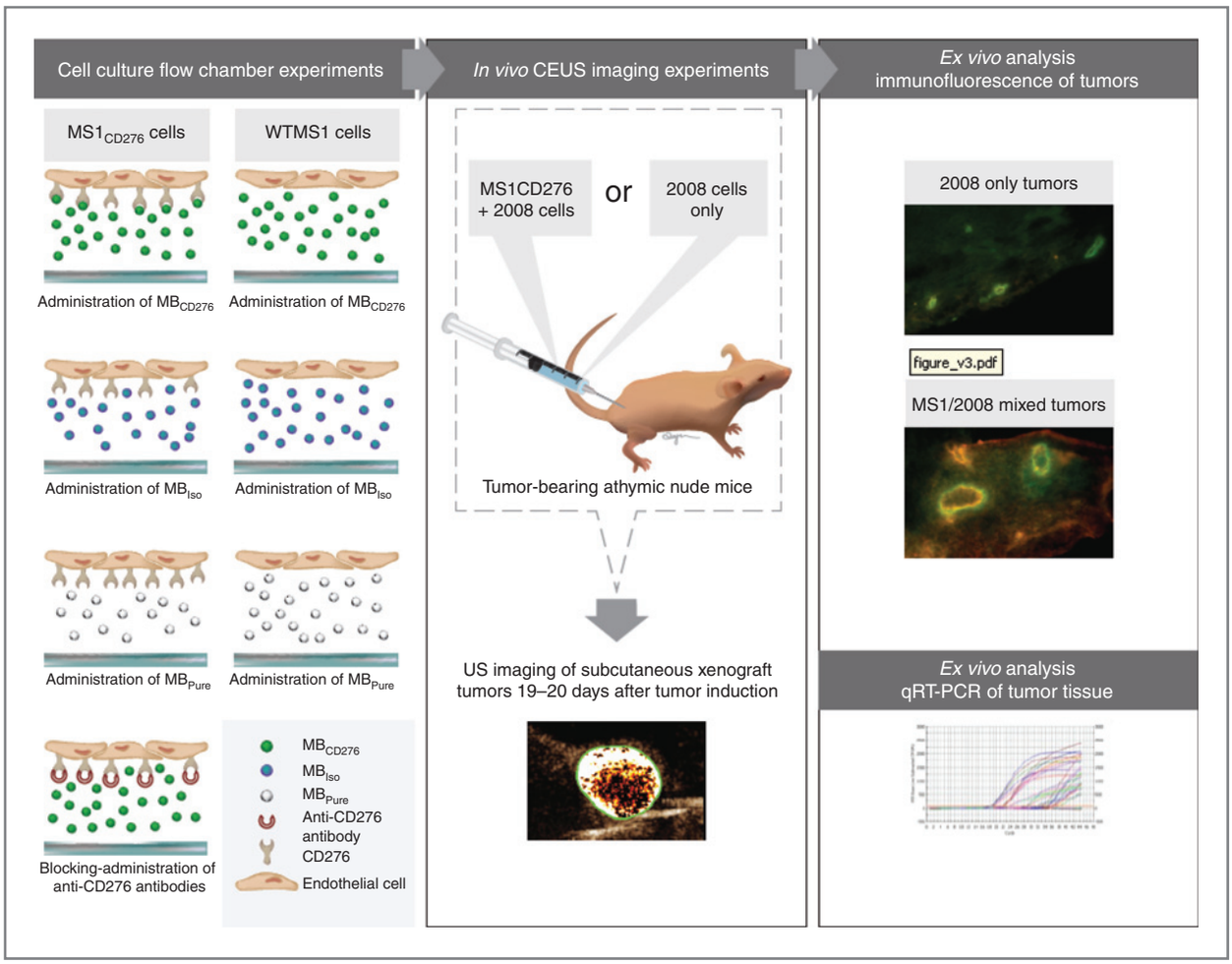

Figure 2. Outline of the experimental algorithm. Binding specificity of MB_{CD276} versus control microbubbles was tested in flow chamber experiments under shear stress conditions comparable to the approximate shear rate in tumor capillaries (100 per second). CD276-expressing engineered MS1 mouse endothelial cells were then coinjected with human 2008 ovarian cancer cells for tumor induction, 2008 only tumors served as control tumors. Both tumor types were used for *in vivo* CEUS imaging 19 to 20 days posttumor induction. *Ex vivo* analysis included immunofluorescence and qRT-PCR of excised tumor tissue.

Ultrasound molecular imaging protocol

Human CD276 binding specificity of MB_{CD276} was tested in 15 mice bearing mixed $MS1_{CD276}$/2008 tumors and in 14 control mice bearing tumors derived from injection of 2008 cells only. To further confirm binding specificity of MB_{CD276} to CD276 in mixed $MS1_{CD276}$/2008 tumors, imaging was repeated after 5 hours following *in vivo* blocking with excess amounts (125 μg) of anti CD276 mAb (eBiosciences) via the tail vein, followed by imaging with MB_{CD276}. For technical details of the ultrasound molecular imaging protocol (see Supplementary Appendix).

In the mixed $MS1_{CD276}$/2008 tumor-bearing mice, 5×10^7 MB_{CD276} or 5×10^7 control MB_{Iso} were injected manually through the tail vein in random order (MB volume, 60 μL per injection; injection time, 3 seconds) during the same imaging session. A minimum time interval of 30 minutes in between injections allowed for clearance of remaining microbubbles from the previous injection (26, 27). To differentiate the acoustic signal derived from microbubbles attached to CD276 on vascular endothelial cells and the signal from freely circulating MBs in the bloodstream, we used the well-established principle of US-induced MB-destruction and replenishment (8, 28). Following the injection of the microbubbles, 4 minutes were allowed for the microbubbles to bind to CD276. One hundred and twenty imaging frames were then captured over a 15-second period to obtain imaging signal from adherent and freely circulating microbubbles in tumor tissue. A continuous high-power destructive pulse of 3.7 MPa (transmit power, 100%; mechanical index, 0.63) was then applied for 1 second, which destroyed the microbubbles within the beam of elevation. Following destruction (15 seconds were given to allow freely circulating microbubbles to refill into tumor vessels), another 120 imaging frames were acquired. The acoustic imaging signals (video intensity) from these 120 imaging frames were averaged digitally subtracted from the

Published OnlineFirst January 3, 2014; DOI: 10.1158/1078-0432.CCR-13-1642

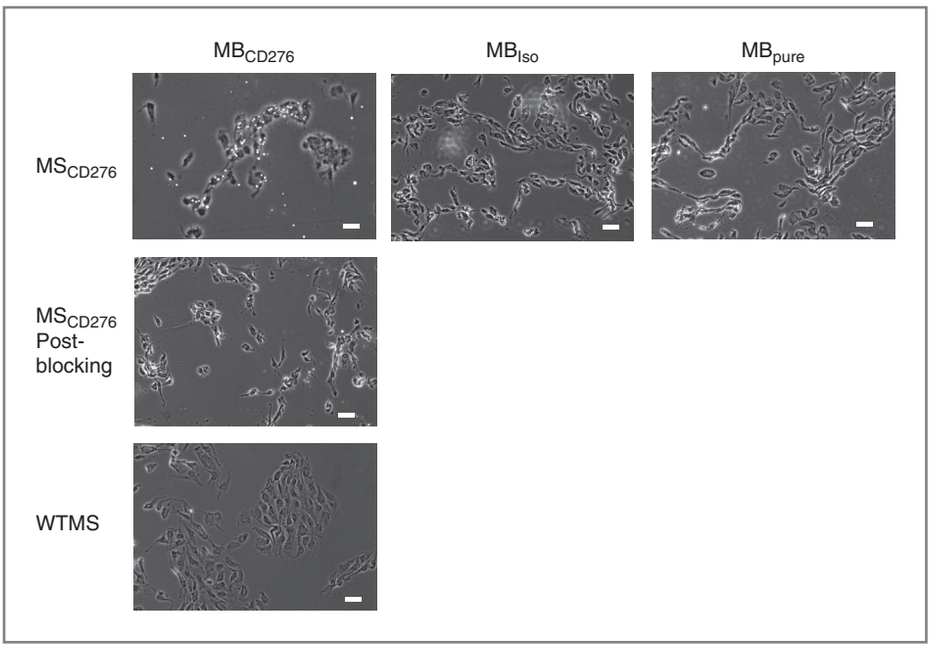

Figure 3. Representative examples of different types of microbubbles (seen as small white dots) binding to CD276-expressing MS1$_{CD276}$ cells and WTMS1 cells in flow chamber attachment experiments. Although many MB$_{CD276}$ attached to MS1$_{CD276}$ cells, control MB$_{Iso}$ and MB$_{pure}$ did not attach to MS1$_{CD276}$ cells. There was a significant reduction of MB$_{CD276}$ attaching to MS1$_{CD276}$ cells after blocking with excess amounts of CD276 mAB and almost no MB$_{CD276}$ attached to WTMS1 cells, which do not express CD276. Scale bar, 10 μm.

initial 120 predestruction frames by the Vevo2100 built-in software. Thus, the calculated difference in video intensity (in linear arbitrary units) corresponded to the imaging signal attributable to CD276 adherent microbubbles (8, 28). Images showing signal from adherent microbubbles were displayed as color maps overlaid on B-mode images, automatically generated by using commercially available Vevo CQ software (VisualSonics).

Imaging data analysis

The imaging datasets of all mice were analyzed offline in random order at a dedicated workstation with commercially available software (VevoCQ; VisualSonics). Analysis was performed in a blinded fashion by one reader, a radiologist with 12 years of experience in reading ultrasound, blinded to the type of microbubble (MB$_{CD276}$ vs. MB$_{Iso}$ or after blocking) and the tumor type (mixed MS1$_{CD276}$/2008 or control 2008 only). Regions of interest were drawn covering the entire area of the subcutaneous tumor and the magnitude of imaging signal from attached microbubble was assessed by calculating an average for pre- and postdestruction imaging signals and subtracting the average postdestruction signal from the average predestruction signal, as described previously (8).

Immunofluorescence staining and analysis of tumors

Immediately following the US imaging sessions, mice were sacrificed and tumors were excised, cut in half at about the level of the US imaging plane direction, embedded in Tissue-Tek OCT (Sakura), and frozen. Tumor tissues were double stained for CD31 as a marker for vascular endothelial cells and for the imaging target CD276 to confirm colocalization of CD276 on CD31-positive tumor-associated vascular endothelial cells (see Supplementary Appendix). Quantitative immunofluorescence analysis with correction for image background was performed by using ImageJ software with the multimeasure plugin (ImageJ, NIH, Bethesda, MD). Microvessel density (MVD) analysis was performed using a standardized protocol (23, 29). The total number of vessels was summed for at least 3 random fields of view (single field of view area, 0.56 μm^2) for each tumor slice, and MVD was calculated as the average number of vessels per field of view area (mm^2).

Real-time reverse-transcription PCR

Because the anti-CD276 mAb cannot differentiate between the human and murine protein versions, parts of the frozen resected xenograft tumors were used for quantitative real-time PCR (qRT-PCR) to confirm the presence of mRNA of the expression-optimized gene encoding for CD276 in the mixed MS1$_{CD276}$/2008 tumors. 2008 only tumors served as negative controls. For this purpose, RNA was extracted from tumors using the RNeasy Plus Kit (Qiagen). The complementary DNA was synthesized from the isolated RNA using the superscript vilo cDNA Synthesis Kit (Life Technologies). For the qRT-PCR, SYBR GreenER qPCR SuperMix universal was used (Life Technologies). All steps were performed following the manufacturers' protocols. qRT-PCR was performed for 3 mixed MS1$_{CD276}$/2008 and for 3 control 2008 only tumors, respectively, using primers for mouse α-tubulin as a reference control gene, for the expression-optimized gene sequence of human *CD276* (see Supplementary Appendix), and for human *CD276* using a commercially available RT-PCR thermal cycler system (Icycler, Bio-Rad). Results were given as cycle threshold (Ct) values and the approximate relative difference in expression according to the ΔΔCt method (30). The Ct value reflects the cycle round when the fluorescence intensity of the samples exceeded a specific threshold, using a threshold

Published OnlineFirst January 3, 2014; DOI: 10.1158/1078-0432.CCR-13-1642

of 150.00 for all tested conditions. A Ct value of ≥40.00 was considered to represent lack of RNA presence.

Statistical analysis

All results are given as mean ± SEM as well as median where appropriate. Comparisons within each tumor of MB_{CD276} signal intensity versus MB_{Iso} signal intensity, and MB_{CD276} signal intensity versus MB_{CD276} signal intensity after blocking were made with 2-sided paired Wilcoxon tests.

Comparisons of MB_{CD276} signal intensity, mean immunofluorescence, and microvessel density in mixed $MS1_{CD276}$/2008 tumors versus control 2008 only tumors were made with a 2-sided unpaired Wilcoxon test. A Bonferroni-adjusted significance level of 0.01 was used for all Wilcoxon tests. Comparison between the different conditions of flow chamber experiments was made with a nonparametric Mann–Whitney *U* test. Statistical analysis was done using Stata Release 9.2 (StataCorp LP).

Results

Flow chamber experiments testing microbubble binding specificity to CD276

The number of MB_{CD276} attaching per cell to $MS1_{CD276}$ cells (1.64 ± 0.18) was significantly higher ($P < 0.001$) compared with the MB_{CD276} attaching to MS1 WT cells (0.22 ± 0.04). Postblocking with excess amounts of anti-CD276 mAb, attachment of MB_{CD276} to $MS1_{CD276}$ cells was significantly reduced to 0.29 ± 0.04 MB_{CD276}/cell ($P < 0.001$). Attachment of control microbubbles to $MS1_{CD276}$ cells was significantly lower, with only a mean of 0.18 ± 0.04/cell for MB_{pure} ($P < 0.001$) and 0.28 ± 0.08/cell for MB_{Iso} ($P < 0.001$) attaching. These findings indicate that the created MB_{CD276} bound specifically to $MS1_{CD276}$ cells expressing human CD276. Examples of different microbubble-type attachments under different conditions in flow chamber experiments are shown in Fig. 3.

Mouse ultrasound imaging

All animals tolerated the CEUS imaging well without signs of any acute toxic reactions after MB administration, and all animals fully recovered after the US imaging sessions.

The binding specificity of MB_{CD276} was tested *in vivo* in 15 mixed $MS1_{CD276}$/2008 tumors and in 14 control 2008 only tumors. US imaging after administration of MB_{Iso} as well as administration of MB_{CD276} after blocking with excess amounts of anti-CD276 mAb served as control conditions for *in vivo* US imaging. The imaging signal of MB_{CD276} was significantly higher in mixed $MS1_{CD276}$/2008 tumors than in control 2008 only tumors with a mean difference in video intensity of 484.95 ± 192.02 versus 52.97 ± 17.6 ($P = 0.006$). The imaging signal of MB_{CD276} in mixed $MS1_{CD276}$/2008 tumors after blocking with excess amounts of anti-CD276 mAb was significantly lower than before blocking with a mean of 272.92 ± 70.49 ($P = 0.0096$). The imaging signal was also significantly lower following administration of MB_{Iso} with a mean difference in video intensity of 252.7 ± 70.49 ($P = 0.002$) in mixed $MS1_{CD276}$/2008 tumors. In 2008 only tumors, imaging signal was also lower after administrating MB_{CD276} following blocking with excess amounts of anti-CD276 mAb with a mean difference in video intensity of 19.33 ± 4.7 ($P = 0.40$) and after administration of MBIso with a mean difference in video intensity of 38.76 ± 14.03 ($P = 0.89$). Although the average signal intensity was lower, contrary to the mixed $MS1_{CD276}$/2008 tumors, there was no consistent drop in signal intensity in all 2008 only tumors under control conditions. Six of fourteen 2008 only tumors had an almost stable signal intensity under control conditions. Figure 4 demonstrates examples of *in vivo* CD276-targeted CEUS.

Ex vivo immunofluorescence analysis

Tumor slices were double stained for human/mouse CD276 and CD31. The mean immunofluorescence of CD276 was significantly higher ($P < 0.001$) in the mixed $MS1_{CD276}$/2008 tumors (mean, 36.82 ± 12.72) than in the control 2008 only tumors (mean, 10.51 ± 4.59). Immunofluorescence double staining showed colocalization of CD276 and CD31 on tumor-associated vascular endothelial cells predominantly in the mixed $MS1_{CD276}$/2008 tumors, to a lesser degree also in the control 2008 only tumors (Fig. 5). The mean vessel density was minimally higher in the mixed $MS1_{CD276}$/2008 tumors with 22.80 vessels/mm^2 than in the control 2008 only tumors with 20.77 vessels/mm^2, but the difference was not statistically significant ($P = 0.54$). Figure 5 demonstrates representative views of stained tumor samples.

Quantitative real-time PCR

qRT-PCR was performed in tumor samples of both tumor types to confirm presence of mRNA deriving from the expression-optimized gene sequence of human *CD276* ($CD276_{engineered}$), which indicates expression of the engineered gene sequence in the tumors. Because the anti-CD276 mAb used in our study cross-reacts with both, the human and mouse CD276 protein, immunofluorescence analysis alone could not differentiate between the 2 protein versions. Relative quantification performed by qRT-PCR confirmed the presence of mRNA deriving from $CD276_{engineered}$ in the mixed $MS1_{CD276}$/2008 tumors, but not in the control 2008 only tumors as reflected by Ct values of 27.98 ± 2.03 in the mixed $MS1_{CD276}$/2008 tumors versus 40.46 ± 2.38 for the control 2008 only tumors, whereas the internal control, mouse α-tubulin, showed comparable Ct values of 20.82 ± 2.38 in the mixed $MS1_{CD276}$ tumors and 21.56 ± 1.39 for the control 2008 only tumors. This resulted in a ΔΔCt value of 11.74 and approximately 3,420-fold more $CD276_{engineered}$ mRNA in the mixed $MS1_{CD276}$/2008 tumors than in the control 2008 only tumors.

Discussion

Extensive research efforts target the molecular footprint of tumor-associated neovasculature and numerous newly discovered angiogenesis markers are explored for their diagnostic or therapeutic suitability. *In vitro* assays are

Published OnlineFirst January 3, 2014; DOI: 10.1158/1078-0432.CCR-13-1642

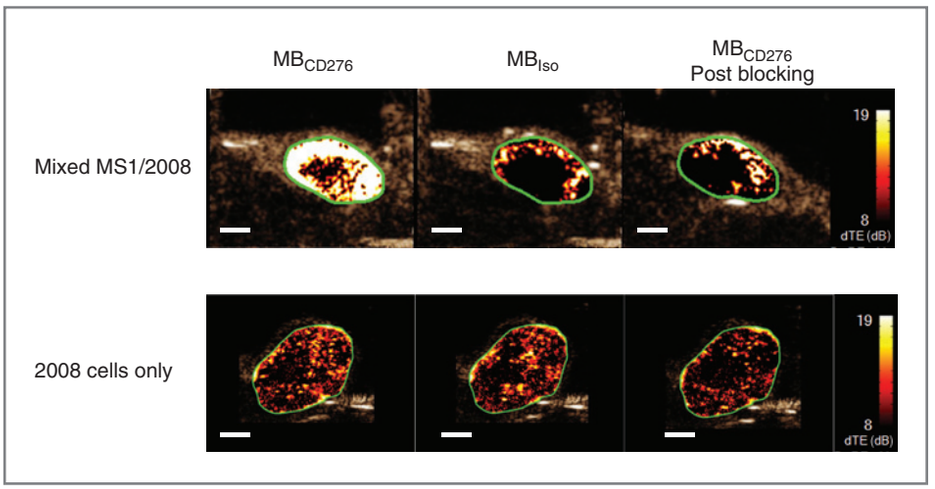

Figure 4. Representative imaging examples of transverse *in vivo* CEUS in mixed MS1$_{CD276}$/2008 tumors and control 2008 only tumors. There is markedly higher imaging signal following injection of MB$_{CD276}$ in mixed MS1$_{CD276}$/2008 tumors as compared with control 2008. Imaging signal was substantially lower after injection of control MB$_{Iso}$ as well as blocking experiments with excess anti CD276 mAb. The decrease of the MBCD276 in 2008 only tumors after blocking with anti-CD276 mAB is explained by the low inherent expression of murine CD276 in those tumors. Scale bar, 1 mm. Note that the antibodies used in these experiments could not differentiate between murine and human CD276, therefore additional qRT-PCR experiments were performed to confirm presence of mRNA deriving from the expression-optimized gene sequence of human *CD276* (*CD276*$_{engineered}$) in mixed MS1$_{CD276}$/2008 tumors (for results see main text). Targeted CEUS imaging signal was color coded and overlaid on contrast-mode gray scale images.

important in the development of novel diagnostic or therapeutic angiogenesis markers, but because of their inherent simplicity they cannot really reflect the complex angiogenesis mechanisms *in vivo*. Small animal models provide an opportunity to study the complex interactions that drive angiogenesis in real time but may be of limited relevance for ultimate clinical translation, because they may lack the expression of specific human angiogenesis markers (31).

This lack of expression led us to implement a relatively simple ovarian cancer animal model that allows modulating the expression of human protein markers on vascular endothelial cells of xenograft tumors in mice and show that the differences in marker expression can be assessed by molecularly targeted CEUS. In this animal model, mouse endothelial cells are transfected with the human angiogenesis marker gene of choice and are coinjected with human cancer cells to induce subcutaneous xenograft tumors in

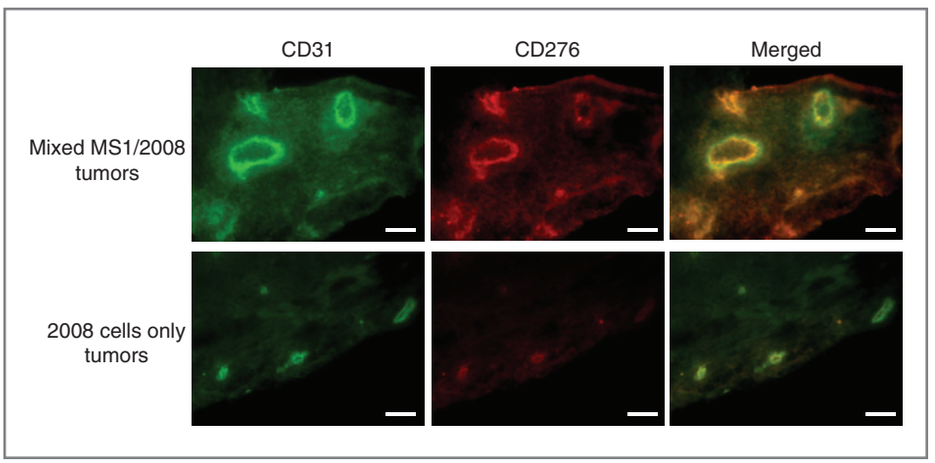

Figure 5. Representative images of tumor immunofluorescence staining demonstrate strong expression of *human* CD276 on the tumor-associated vasculature in the mixed MS1/2008 tumors (top row) as indicated by the strong orange color change on the merged images. Low background expression of *murine* CD276 is seen on the tumor-associated vasculature in control 2008 only tumors (bottom row) with only some vessels showing expression of CD276 as indicated by the orange color on merged images whereas other vessels remain green showing no CD276 expression. Note that the antibodies used in these experiments could not differentiate between murine and human CD276, therefore additional qRT-PCR experiments were performed to confirm presence of mRNA deriving from the expression-optimized gene sequence of human *CD276* (*CD276*$_{engineered}$) in mixed MS1/2008 tumors (for results see main text). Scale bar, 20 μm.

Published OnlineFirst January 3, 2014; DOI: 10.1158/1078-0432.CCR-13-1642

nude mice. In our case, MS1 mouse vascular endothelial cells were transfected with an expression optimized gene of human *CD276* and the stable CD276-expressing cells were coinjected with human 2008 ovarian cancer cells to induce xenograft tumors whereas typically used tumors induced by injection of 2008 cells only served as negative controls. The expression of human CD276 on the surface of the engineered $MS1_{CD276}$ endothelial cells was first proven by flow chamber cell attachment studies where $MS1_{CD276}$ and WT MS1 cells were exposed to CD276-targeted as well as control microbubbles under shear stress conditions comparable to those of tumor capillaries. The *in vivo* upregulation of human CD276 expression on tumor-associated vascular endothelial cells in the mixed $MS1_{CD276}$/2008 tumors was proven by immunofluorescence analysis of harvested tumor tissue where a more than 3-fold higher average CD276 fluorescence signal was observed as compared with the control 2008 only tumors. The vessel density, however, was comparable for both tumor types. This indicates that the higher CD276 fluorescence signal in the mixed $MS1_{CD276}$/2008 tumors cannot be simply explained by a higher vessel density or vessel surface area in those mixed tumors. Furthermore, the difference in CD276 expression in both tumor types could be assessed by *in vivo* CD276-targeted CEUS. These *in vivo* ultrasound studies showed significantly higher imaging signal in mixed $MS1_{CD276}$/2008 tumors following administration of MB_{CD276} compared with control 2008 only tumors. Furthermore, the specificity of MB_{CD276} binding to tumor-associated vessels in mixed $MS1_{CD276}$/2008 tumors *in vivo* was demonstrated by the significant imaging signal reduction deriving from MB_{CD276} following blocking with excessive amounts of monoclonal anti-CD276 antibody. The imaging signal deriving from MB_{Iso} in mixed $MS1_{CD276}$/2008 tumors was also significantly lower when compared with that deriving from MB_{CD276} in those mixed tumors; interestingly, however, the imaging signal following administration of MB_{Iso} in the mixed $MS1_{CD276}$/2008 tumors was relatively high, indicating that there may have been nonspecific binding of the isotype-matched control antibody to vascular endothelial cells in the modified mixed tumors. Another potential explanation for part of the nonspecific binding effect may be a nonspecific interaction of streptavidin on the microbubble surface with mouse endogenous fibronectin (32). Another observation was that there was specific attachment of MB_{CD276} in 2008 only tumors, indicating some expression of murine CD276 in those tumors, which was detectable by MB_{CD276} because the anti-CD276 antibody used to functionalize the microbubbles cross-reacts with both human and murine CD276.

CD276 was chosen as an imaging target because it may be of high clinical value in the therapeutic and diagnostic setting of ovarian cancer (14–17). To date, several molecularly targeted CEUS imaging studies have focused on VEGFR2, which is known to be overexpressed in numerous tumors (7–11). In patients with premenopausal ovarian cancer, however, VEGFR2 could be a less optimal US imaging target, because it is not a cancer-specific angiogenesis marker, although ovarian cancer occurs in postmenopausal patients in the vast majority of cases where VEGFR2 may be a highly suitable imaging target. Expression of VEGFR2 is known to be upregulated on vascular endothelial cells at sites of wound healing, which also regularly occurs in the ovary in the early luteal phase following ovulation: the cyclic corpus luteum of the ovary is known to be the organ site with the strongest physiologic angiogenesis (13, 33). Therefore, a valid concern is that imaging strategies targeting VEGFR2 may detect physiologic angiogenesis associated with ovulation in premenopausal women, although further studies in patients are warranted to corroborate this hypothesis. An ideal vascular marker candidate for molecularly targeted ultrasound in ovarian cancer should be highly overexpressed in cancer-associated endothelial cells *and* not or only to limited extent expressed in endothelial cells from site matched normal vessels and at sites of physiologic angiogenesis, known to encode for membrane proteins with luminal sided surface expression and have a biologic function potentially related to angiogenesis.

CD276 (B7-H3), a member of the immunoglobulin superfamily, has just recently been identified as one vascular endothelial target that may possess most of the desired vascular marker qualities for ovarian cancer (16, 17). As an immune regulatory ligand CD276 is thought to attenuate peripheral immune responses and its overexpression in tumors, therefore, to be associated with poor prognosis (16). CD276 is overexpressed not only on tumor cells, but also on tumor-associated vascular endothelial cells in ovarian cancer and the level of CD276 expression has been shown to be associated with tumor histology (most often expressed in serous ovarian carcinomas) and stage (16). These findings were also reflected by the results of immunohistochemical validation of CD276 as a vascular endothelial target in a tissue filter set consisting of 15 high-grade serous ovarian cancer tissue samples, 14 corpus luteum samples, 15 normal ovary samples, 19 benign ovarian disease samples, and 18 samples containing normal fallopian tube endothelium, one of the coauthors could show very favorable performance of CD276 in comparison to VEGFR2: although both markers were highly expressed in blood vessels of high-grade serous ovarian cancer compared with normal and benign ovarian tissue, CD276 was markedly lower expressed (only 50% of the vessel staining composite score of VEBGFR2) in normal fallopian tube endothelium and corpus luteum (C. Drescher et al., unpublished data). Validation of CD276 as a vascular marker of ovarian cancer in larger series of human early stage and occult ovarian cancer tissue samples including analysis by outside laboratories is currently under way. Ultimately, CD276 could serve as 1 of 2 or even 3 complementary cancer-specific imaging targets that may be addressed simultaneously by a multivalent targeted microbubble for ovarian cancer early detection (7, 34).

Because small animal models are a requisite for the development of novel drugs, including contrast agents and

Published OnlineFirst January 3, 2014; DOI: 10.1158/1078-0432.CCR-13-1642

molecular imaging probes (35), we were aiming to develop a CD276-targeted US imaging strategy, but were hampered by the relative low levels of CD276 expression in our small animal ovarian cancer models as compared with human cancers. Following the concept that endothelial cells can form tubular three-dimensional structures that can connect to host capillary microcirculation (20), we attempted to create an animal model that allows influencing the expression level of human vascular imaging targets on tumor-associated vascular endothelial cells in a mouse host to be able to develop novel imaging probes and imaging strategies addressing these human vascular targets. Animal models with humanized vasculature have been explored by several authors to study the complex mechanisms of angiogenesis *in vivo* (20, 36). Other models using, for example, human umbilical vein endothelial cells (HUVEC) offer the advantage of including the entire human endothelial cells as compared with expression of just one human marker protein as in our animal model. The disadvantage of those models however is that for optimal results they may require more elaborate three-dimensional culture techniques and typically severe combined immunodeficiency mice hosts as well as that HUVEC cells usually require more elaborate approaches for gene expression such as lentivirus transduction. In addition, gene expression of specific target proteins can be quite challenging in primary HUVECs.

We acknowledge the following limitations of our study. First, we used streptavidin-coated microbubbles that can be functionalized in the laboratory setting, but are not suitable for use in patients. Second, we tested the CD276-targeted US imaging strategy only in ovarian cancer models and not in models of benign ovarian disease. Third, although CD276 may be a promising imaging target for a multitargeted US imaging approach in ovarian cancer early detection, the exact mechanism of the CD276 molecule in tumor angiogenesis is unclear to date. Finally, our model may not assess the true signal to noise ratio expected in patients, because overexpression of CD276 on murine endothelial cells may not reflect magnitude of CD276 expression levels in patients. However, our model is primarily meant to facilitate expression of human vascular targets on tumor-associated vascular endothelial cells in a small animal host for the initial *in vivo* testing of novel imaging or therapeutic approaches and, therefore, our relatively simple mouse model may prove to be a cost-effective and robust method which can be applied in a high-throughput multiuser lab environment.

In conclusion, we have shown that the proposed animal model allows modulation of the expression of a human ovarian cancer–associated vascular target, such as CD276 on tumor-associated vascular endothelial cells in the mouse host and that these differences in CD276 expression on vascular endothelial cells can be assessed with molecularly targeted US imaging. Although we have not yet tested this approach in a second ovarian tumor model, we are convinced that this novel small animal model may be applicable to many other human vascular targets and the ability to visualize target expression differences via molecularly targeted CEUS may facilitate not only the development of imaging probes addressing upcoming vascular imaging targets for cancer imaging, but may also be helpful in the development of novel therapeutics addressing those vascular targets.

Disclosure of Potential Conflicts of Interest

J.K. Willmann is a consultant for Bracco. S.S. Gambhir is a consultant/advisory board member for Bracco and VisualSonics. No potential conflicts of interest were disclosed by the other authors.

Authors' Contributions

Conception and design: A.M. Lutz, C.W. Drescher, J.K. Willmann, S.S. Gambhir
Development of methodology: A.M. Lutz, S.V. Bachawal, J.K. Willmann, S.S. Gambhir
Acquisition of data (provided animals, acquired and managed patients, provided facilities, etc.): A.M. Lutz, S.V. Bachawal, M.A. Pysz, J.K. Willmann
Analysis and interpretation of data (e.g., statistical analysis, biostatistics, computational analysis): A.M. Lutz, J.K. Willmann, S.S. Gambhir
Writing, review, and/or revision of the manuscript: A.M. Lutz, S.V. Bachawal, C.W. Drescher, M.A. Pysz, J.K. Willmann, S.S. Gambhir
Administrative, technical, or material support (i.e., reporting or organizing data, constructing databases): J.K. Willmann, S.S. Gambhir
Study supervision: J.K. Willmann, S.S. Gambhir

Acknowledgments

The authors thank J. Rosenberg, Ph.D., for his help with the statistical analysis and George Coukos, M.D., Ph.D. for valuable discussions and advice about the animal model.

Grant Support

This work is supported in part by the NIH P50 CA083636 SPORE grant (S.S. Gambhir, A.M. Lutz, J.K. Willmann), Marsha Rivkin Center for Ovarian Cancer Research Scholar Award (A.M. Lutz), R01 CA155289-01A1 (J.K. Willmann), and Canary Foundation (S.S. Gambhir, J.K. Willmann, C.W. Drescher).

The costs of publication of this article were defrayed in part by the payment of page charges. This article must therefore be hereby marked *advertisement* in accordance with 18 U.S.C. Section 1734 solely to indicate this fact.

Received June 14, 2013; revised December 4, 2013; accepted December 17, 2013; published OnlineFirst January 3, 2014.

References

1. Siegel R, Naishadham D, Jemal A. Cancer statistics, 2012. CA: Cancer J Clin 2012;62:10–29.
2. Del Carmen MG. Primary epithelial ovarian cancer: diagnosis and management. Am Soc Clin Oncol Educ Book 2006;330–334.
3. Chan JK, Cheung MK, Husain A, Teng NN, West D, Whittemore AS, et al. Patterns and progress in ovarian cancer over 14 years. Obstet Gynecol 2006;108:521–8.
4. van Nagell JR Jr., DePriest PD, Ueland FR, DeSimone CP, Cooper AL, McDonald JM, et al. Ovarian cancer screening with annual transvaginal sonography: findings of 25,000 women screened. Cancer 2007;109:1887–96.
5. Lutz AM, Willmann JK, Drescher CW, Ray P, Cochran FV, Urban N, et al. Early diagnosis of ovarian carcinoma: is a solution in sight? Radiology 2011;259:329–45.

Published OnlineFirst January 3, 2014; DOI: 10.1158/1078-0432.CCR-13-1642

6. Buys SS, Partridge E, Black A, Johnson CC, Lamerato L, Isaacs C, et al. Effect of screening on ovarian cancer mortality: the Prostate, Lung, Colorectal and Ovarian (PLCO) Cancer Screening Randomized Controlled Trial. JAMA 2011;305:2295–303.
7. Willmann JK, Lutz AM, Paulmurugan R, Patel MR, Chu P, Rosenberg J, et al. Dual-targeted contrast agent for US assessment of tumor angiogenesis *in vivo*. Radiology 2008;248:936–44.
8. Willmann JK, Paulmurugan R, Chen K, Gheysens O, Rodriguez-Porcel M, Lutz AM, et al. US imaging of tumor angiogenesis with microbubbles targeted to vascular endothelial growth factor receptor type 2 in mice. Radiology 2008;246:508–18.
9. Bzyl J, Lederle W, Rix A, Grouls C, Tardy I, Pochon S, et al. Molecular and functional ultrasound imaging in differently aggressive breast cancer xenografts using two novel ultrasound contrast agents (BR55 and BR38). Eur Radiol 2011;21:1988–95.
10. Lee DJ, Lyshchik A, Huamani J, Hallahan DE, Fleischer AC. Relationship between retention of a vascular endothelial growth factor receptor 2 (VEGFR2)-targeted ultrasonographic contrast agent and the level of VEGFR2 expression in an *in vivo* breast cancer model. J Ultrasound Med 2008;27:855–66.
11. Deshpande N, Ren Y, Foygel K, Rosenberg J, Willmann JK. Tumor angiogenic marker expression levels during tumor growth: longitudinal assessment with molecularly targeted microbubbles and US imaging. Radiology 2011;258:804–11.
12. Bzyl J, Palmowski M, Rix A, Arns S, Hyvelin JM, Pochon S, et al. The high angiogenic activity in very early breast cancer enables reliable imaging with VEGFR2-targeted microbubbles (BR55). Euro Radiol 2013;23:468–75.
13. Sugino N, Kashida S, Takiguchi S, Karube A, Kato H. Expression of vascular endothelial growth factor and its receptors in the human corpus luteum during the menstrual cycle and in early pregnancy. J Clin Endocrinol Metab 2000;85:3919–24.
14. Buckanovich RJ, Sasaroli D, O'Brien-Jenkins A, Botbyl J, Hammond R, Katsaros D, et al. Tumor vascular proteins as biomarkers in ovarian cancer. J. Clin Oncol 2007;25:852–61.
15. Sasaroli D, Gimotty PA, Pathak HB, Hammond R, Kougioumtzidou E, Katsaros D, et al. Novel surface targets and serum biomarkers from the ovarian cancer vasculature. Cancer Biol Ther 2011;12:169–80.
16. Zang X, Sullivan PS, Soslow RA, Waitz R, Reuter VE, Wilton A, et al. Tumor associated endothelial expression of B7-H3 predicts survival in ovarian carcinomas. Modern Pathol 2010;23:1104–12.
17. Seaman S, Stevens J, Yang MY, Logsdon D, Graff-Cherry C, St Croix B. Genes that distinguish physiological and pathological angiogenesis. Cancer Cell 2007;11:539–54.
18. Crispen PL, Sheinin Y, Roth TJ, Lohse CM, Kuntz SM, Frigola X, et al. Tumor cell and tumor vasculature expression of B7-H3 predict survival in clear cell renal cell carcinoma. Clin Cancer Res 2008;14:5150–7.
19. Brunner A, Hinterholzer S, Riss P, Heinze G, Brustmann H. Immunoexpression of B7-H3 in endometrial cancer: relation to tumor T-cell infiltration and prognosis. Gynecol Oncol 2012;124:105–11.
20. Laib AM, Bartol A, Alajati A, Korff T, Weber H, Augustin HG. Spheroid-based human endothelial cell microvessel formation *in vivo*. Nat Protocols 2009;4:1202–15.
21. Lipofectamine 2000 Reagent Manual [cited 2014 Jan 2]. Available from: http://tools.lifetechnologies.com/content/sfs/manuals/Lipofectamine_2000_Reag_protocol.pdf.
22. Pysz MA, Foygel K, Rosenberg J, Gambhir SS, Schneider M, Willmann JK. Antiangiogenic cancer therapy: monitoring with molecular US and a clinically translatable contrast agent (BR55). Radiology 2010;256:519–27.
23. Weidner N. Chapter 14: Measuring intratumoral microvessel density. Methods Enzymol 2008;444:305–23.
24. Shaw TJ, Senterman MK, Dawson K, Crane CA, Vanderhyden BC. Characterization of intraperitoneal, orthotopic, and metastatic xenograft models of human ovarian cancer. Mol Ther 2004;10:1032–42.
25. Arbiser JL, Moses MA, Fernandez CA, Ghiso N, Cao Y, Klauber N, et al. Oncogenic H-ras stimulates tumor angiogenesis by two distinct pathways. Proc Natl Acad Sci USA 1997;94:861–6.
26. Weller GE, Wong MK, Modzelewski RA, Lu E, Klibanov AL, Wagner WR, et al. Ultrasonic imaging of tumor angiogenesis using contrast microbubbles targeted via the tumor-binding peptide arginine-arginine-leucine. Cancer Res 2005;65:533–9.
27. Willmann JK, Cheng Z, Davis C, Lutz AM, Schipper ML, Nielsen CH, et al. Targeted microbubbles for imaging tumor angiogenesis: assessment of whole-body biodistribution with dynamic micro-PET in mice. Radiology 2008;249:212–9.
28. Kaufmann BA, Carr CL, Belcik JT, Xie A, Yue Q, Chadderdon S, et al. Molecular imaging of the initial inflammatory response in atherosclerosis: implications for early detection of disease. Arterioscler Thromb Vasc Biol 2010;30:54–9.
29. Guidi AJ, Fischer L, Harris JR, Schnitt SJ. Microvessel density and distribution in ductal carcinoma in situ of the breast. J Natl Cancer Inst 1994;86:614–9.
30. Livak KJ, Schmittgen TD. Analysis of relative gene expression data using real-time quantitative PCR and the $2(-\Delta\Delta C(T))$ method. Methods 2001;25:402–8.
31. Teicher BA. Tumor models for efficacy determination. Mol Cancer Ther 2006;5:2435–43.
32. Klibanov AL, Rasche PT, Hughes MS, Wojdyla JK, Galen KP, Wible JHJr., et al. Detection of individual microbubbles of an ultrasound contrast agent: fundamental and pulse inversion imaging. Acad Radiol 2002;S279–81.
33. Augustin HG. Vascular morphogenesis in the ovary. Bailliere's Best Prac Res Clin Obstet Gynaecol 2000;14:867–82.
34. Urban N, McIntosh MW, Andersen M, Karlan BY. Ovarian cancer screening. Hematol Oncol Clin North Am 2003;17:989–1005, ix.
35. Willmann JK, van Bruggen N, Dinkelborg LM, Gambhir SS. Molecular imaging in drug development. Nat Rev Drug Discovery 2008;7:591–607.
36. Alajati A, Laib AM, Weber H, Boos AM, Bartol A, Ikenberg K, et al. Spheroid-based engineering of a human vasculature in mice. Nat Methods 2008;5:439–45.

Published OnlineFirst January 3, 2014; DOI: 10.1158/1078-0432.CCR-13-1642

Clinical Cancer Research

Ultrasound Molecular Imaging in a Human CD276 Expression–Modulated Murine Ovarian Cancer Model

Amelie M. Lutz, Sunitha V. Bachawal, Charles W. Drescher, et al.

Clin Cancer Res 2014;20:1313-1322. Published OnlineFirst January 3, 2014.